Influence of Nonhorizontal Orientation on Measurement of Insect Biological Parameters With Entomological Radar

Weidong Li, Cheng Hu, *Senior Member, IEEE*, Rui Wang, Muyang Li, Fan Zhang, and Jiangtao Wang

***Abstract*— Up till now, measurement of the biological parameters of insects traversing the beam of an entomological radar has been based on the assumption that the insects maintain a horizontal flight attitude. However, recent studies have revealed that some migrating insects fly with their bodies pitched upwards. This article analyzes the influence of nonhorizontal orientation (i.e., pitch and roll angles) on measurements of insect biological parameters with an entomological radar. The scattering matrices (SMs) of 15 insect specimens have been measured at different pitch and roll angles with a purpose-designed multiaspect fully polarimetric laboratory rig. It is found that pitch angle has little influence on the discrimination of "parallel" and "perpendicular" insects, but it affects the measurement accuracy of orientation and estimation of mass and body length. The roll angle has little influence on the insect class discrimination, and the measurement of orientation and body length, and slightly affects the accuracy of the mass estimation. The influence of a general combination of pitch and roll angles is approximately the linear superposition of the influence of pitch angle and roll angle.**

***Index Terms*—Biological parameter estimation, entomological radar, insect, pitch angle, roll angle.**

I. Introduction

EVERY year, countless numbers of migratory insects cross the planet in pursuit of increased foraging opportunities, improved safety, and higher reproductive output [1]. Insect migration represents the most important annual animal movement in terrestrial ecosystems [2]. In terms of total moving biomass, the migrations of individual insect species rival and sometimes outstrip the largest extant herds and flocks of some well-known migratory mammals and birds [3]. These bioflows lead to huge seasonal exchanges of biomass and nutrients across Earth's surface [2]. However, the behavioral adaptations that facilitate these movements remain largely unknown [4]. To find out the ultimate reasons and proximate mechanisms that would explain these mass movements, a quantitative observing system for monitoring insect migration is required.

Radar was developed before and during the Second World War for detecting and tracking aircraft and ships, and it was subsequently applied to monitoring weather [5]. However, with the advent of microwave radar, point targets, called "dot angels," were often detected in apparently clear air, to the puzzlement of radar engineers and meteorologists until it was verified that the echo signals were from flying insects [6], [7]. Since then, radar (both purpose-built entomological units and more recently weather radars) has been used by entomologists to study insect migration, and has become one of the most effective tools for observing insect flight [8]–[15].

Early purpose-built entomological radars employed a scanning pencil-beam configuration [8]. The radar observations were displayed on a plan position indicator and recorded by photographing. The photographs were then used for data processing that, with the technology then available, was very time-consuming, making this type unsuitable for routine long-term monitoring [9]. In addition, the sloping and moving beam provided limited capability for measuring the insect biological parameters needed to identify the type of insect being observed. Since the late 1990s, entomological radars employing a vertical beam through which insects pass have largely displaced scanning systems. The ZLC (Zenith-pointing linear-polarized conical scan) configuration, in which the polarization is rapidly rotated in synchrony with a very small angle scan, is particularly favored, with implementations known either as insect monitoring radars (IMRs) or vertical-looking radars (VLRs). These provide long-term observations fully automatically and allow estimation of the orientation, mass, wing-beat frequency, and speed of individual insects [11]–[17]. These parameters are valuable for identifying the species and studying the behaviors of migratory insects. The IMRs and VLRs use noncoherent radar technology, but coherent and fully polarimetric entomological radars have now been developed [18]. Studies of the application of coherence and full polarization to measurement of the radar

Manuscript received 8 February 2022; revised 13 April 2022 and 19 May 2022; accepted 26 June 2022. Date of publication 28 June 2022; date of current version 12 July 2022. This work was supported in part by the Special Fund for Research on National Major Research Instruments under Grant 31727901, in part by the Major Scientific and Technological Innovation Project of Shandong Province under Grant 2020CXGC010802, and in part by the National Natural Science Foundation of China under Grant 62001021. *(Corresponding author: Cheng Hu.)*

Weidong Li, Cheng Hu, and Rui Wang are with the Radar Research Lab, School of Information and Electronics, Beijing Institute of Technology, Beijing 100081, China, and also with the Advanced Technology Research Institute, Beijing Institute of Technology, Jinan 250300, China (e-mail: lwd0539@163.com; hucheng.bit@gmail.com; bit.wangrui@gmail.com).

Muyang Li, Fan Zhang, and Jiangtao Wang are with the Radar Research Lab, School of Information and Electronics, Beijing Institute of Technology, Beijing 100081, China, and also with the Key Laboratory of Electronic and Information Technology in Satellite Navigation (Beijing Institute of Technology), Ministry of Education, Beijing 100081, China (e-mail: muyangli_bit@163.com; 727752423@qq.com; 1278300736@qq.com).

Digital Object Identifier 10.1109/JSTARS.2022.3187034

properties of insects showed that use of these techniques can improve the accuracy of orientation measurements and mass estimates, enable body-length estimation, and discriminate between "parallel" (PA) and "perpendicular" (PE) insects (see below) [19]–[22]. Coherent and fully polarimetric signal processing is expected to be adopted for the next generation of entomological radars [11]. In addition, studies to estimate insect body length and mass based on the multifrequency radar cross-section (RCS) characteristics of insect and machine learning methods were being explored [23]–[25].

The basic target data that a ZLC radar can provide is the variation of the RCS with the direction of linear polarization. This can be considered as the product of a "polarization pattern" (the form of the variation and its alignment) and a polarization-averaged RCS (denoted a_0). The insect orientation can be estimated from the polarization pattern based on the assumption that the RCS reaches its maximal value, while the polarization direction of the radar antenna is parallel to the insect body axis, i.e., that the target is a PA insect [26]. If the target is a PE insect (for which the RCS reaches its maximal value when the polarization direction of the radar antenna is perpendicular to the insect body axis), an orientation error of 90° will arise if the PA assumption is made [21]. More accurately, the "orientation" measured with an IMR is the maximum RCS direction (MRD) of the polarization pattern rather than the insect body axis. To obtain the real orientation, the insect class (PA or PE) needs to be discriminated.

The form of the polarization pattern is characterized by two parameters α_2 and α_4, the magnitudes of two harmonic modulations; α_2 represents the elongation of the pattern and α_4 a cruciform component [20]–[27]. The RCS parameters a_0 and α_2 can be used to estimate the insect mass with the assumption—supported by laboratory measurements—that the insect RCSs increase monotonically with mass at X-band (i.e., that the scattering of insects at X-band is in the Rayleigh or the beginning of the resonance region) [28].

The basic target data that a fully polarimetric radar provides is the scattering matrix (SM). As the polarization pattern is uniquely determined by the SM and can be derived from it, all the information estimated from the polarization pattern can be directly derived from the SM [26]. Thus, the orientation and mass measurement methods for the IMRs are also applicable to the fully polarimetric radar. In addition, the SM can also provide a phase angle $\Delta\phi$ that is lost when the polarization pattern is calculated. This extra information helps to improve the measurement ability of a ZLC entomological radar. $\Delta\phi$, the relative phase of the SM eigenvalues, can be used to discriminate PA and PE insects with a high correct rate [21]. The dominant eigenvector of the SM can be used to estimate the insect MRD with better performance at low signal-to-noise ratio (SNR) than the traditional method [19]. It was also found that ν and d, the invariant target parameters of the SM, can be used to estimate the insect body length and mass with good performance [20].

Up till now, all the estimation methods for insect biological parameters have been based on the assumption that the insects maintained a horizontal flight attitude as they passed through the radar beam [21]–[29]. However, recent studies with dual-polarization weather radars have revealed that some migrating insects fly with their bodies pitched upwards [30], [31]. Because the RCS and polarization characteristics of radar targets are functions of the target aspect, the pitch angle can be expected to affect the basic target data measured by the entomological radar, and introduce bias into the biological parameters estimates. However, there are no published studies of the influence of pitch angle as well as the roll angle on radar estimation of insect biological parameters.

In this article, use of a purpose-designed multiaspect coherent fully polarimetric laboratory rig to measure the SMs of 15 insect specimens at different pitch and roll angles is described. The relationships between the pitch and roll angles and the insect class (PA and PE), the RCS parameters (ν, d, a_0, and α_2), and the relative phase $\Delta\phi$ are examined. The influences of pitch and roll angles on discrimination of PA and PE insects, MRD measurement, and estimation of insect mass and body length are analyzed. The pitch angle and roll angle are two variables. In order to control the variables, the analysis will be divided into cases of pitch angle only, roll angle only, and the combination of pitch angle and roll angle.

All the abbreviations of scientific terms and their definitions in this article are collected in Appendix I in alphabetical order.

II. Polarimetric Measurement Rig

During September 11–20, 2019, insect SM measurements at different pitch and roll angles were made using a multiaspect fully polarimetric rig in a microwave anechoic chamber. The main components of the rig include a fully polarimetric measurement system, a multiaspect support device for the antennas [Fig. 1(a)], and a target support system comprising a polyethylene line between two support rods. The measurement scenario is shown in Fig. 1(b). The fully polarimetric measurement system consists of a four-port vector network analyzer (R&SZVA 40, Rohde & Schwarz, Germany) and two dual-polarized X-band horn antennas. One antenna is used for transmitting and the other for receiving. Each of the horn antennas has H- and V-polarization ports. Ports 1 and 3 of the vector network analyzer were connected to the H- and V-polarization ports of the transmitting antenna, respectively, and ports 2 and 4 to the H- and V-polarization ports of the receiving antenna. The S-parameters S21, S23, S41, and S42 were obtained, corresponding to the HH, HV, VH, and VV polarization echo signals, respectively. See [21] and [32] for further details.

The structure of the multiaspect antennas support device is shown in Fig. 1(a). The main body of the device is a track in the form of a circular arc. Other metal structures support the track. The electromagnetic absorbing material was used to mitigate the potential clutter from these support rods. The radius of the arc is 2 m. On the track, the antenna pedestals are set every 15° from elevation 0° to 75° [the reference 0° is defined as the position directly below the center of the circle on the track, as shown in Fig. 1(a)]. In the measurement, the insect specimen was suspended in the center of the circle through a low-scattering polyethylene line, and its main axis was set parallel to the horizontal plane. The ranges from the insect to all the antenna positions are identical.

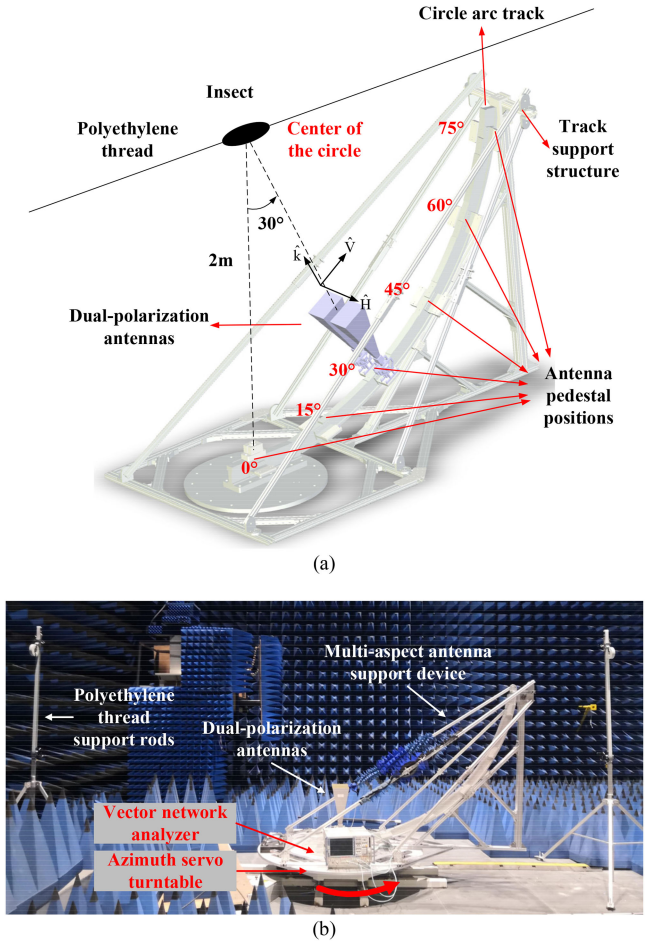

Fig. 1. Insect SM measurements for different pitch and roll angles conducted in a microwave anechoic chamber with a multiple-aspect fully polarimetric rig. (a) Multiaspect antenna support device; $\hat{k}$, $\hat{H}$, and $\hat{V}$ represent the directions of radiation, H-polarization, and V-polarization, respectively. (b) Equipment setup in anechoic chamber.

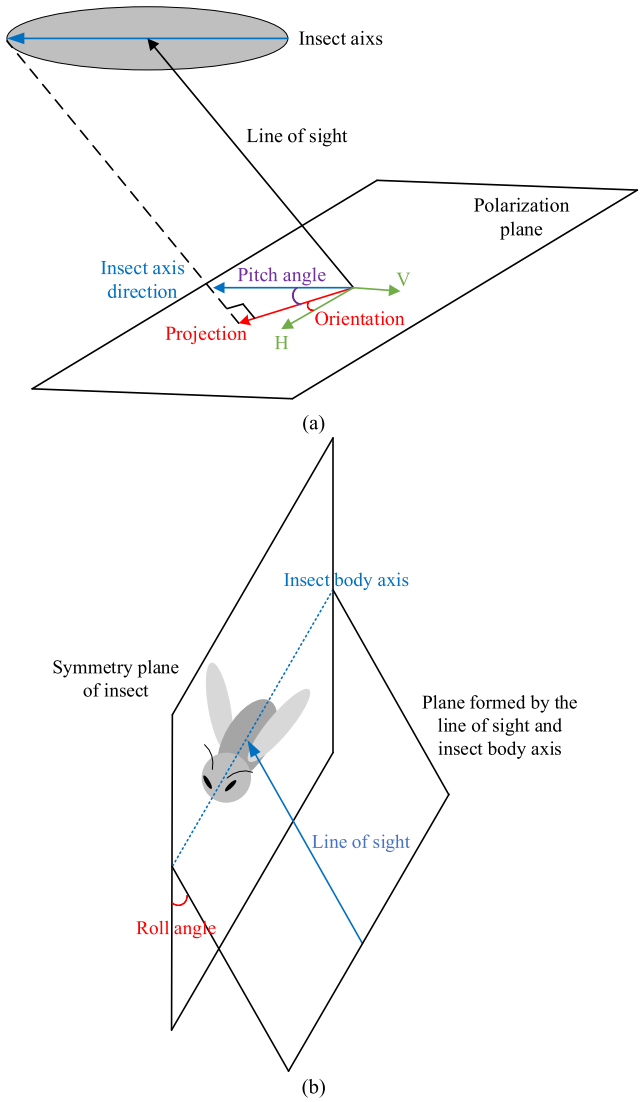

Fig. 2. Diagrammatic sketches of (a) pitch angle and orientation, and (b) roll angle.

The track was mounted on a high precision azimuth servo turntable [Fig. 1(b)]. By rotating the turntable, the azimuth of the track can be adjusted. The reference 0° of the track azimuth is defined as the direction of the insect's body axis [Fig. 1(a)]. Thereby, the positions of the antennas can move on a lower hemisphere with a radius of 2 m, and the insect specimen is fixed on the center of the sphere. Thus, the insects can be measured with different combinations of elevation and azimuth of incident radar wave. This simulates the measurement of insects at different pitch and roll angles.

The pitch and roll angles could also be adjusted by keeping the antennas vertical and varying the pitch and roll angles of the polyethylene line. However, in that case, it is difficult to accurately adjust the pitch and roll angles of insect because the polyethylene line is flexible and sags due to gravity. Hence, the method employing the circular track was adopted.

The pitch angle is the angle between the body axis and the polarization plane (i.e., the plane formed by H- and V-polarization vectors, and perpendicular to the line of sight of the antennas), as shown in Fig. 2(a). When the azimuth of the antennas is 0°, the pitch angle is equal to the elevation of the antennas position. Thus, measurement at pitch angles of 0°, 15°, …, and 75° is possible with this system. The roll angle is the angle between the symmetry plane of insect body and the plane formed by the line of sight of radar and insect body axis [Fig. 2(b)]. When the azimuth is 90°, the roll angle is equal to the elevation of the antennas position.

In the measurement, the initial azimuth is 0°. A vertical-plane laser scan was used to ensure that the two support rods, the track, and the center of the circle are in the same plane. A 2-m-long vertical rod can be installed at the center of the 0° pedestal position prior to making a measurement to indicate the center of the circle during setup. The insect's back was stuck to the polyethylene line with super glue, with the body axis parallel to the line. By adjusting the height of the support rods, the polyethylene line could be made to pass through the center of the circle and the insect could then easily be placed there.

The insect specimens used in the experiment were captured by a light trap the night before the measurement. To avoid

TABLE I
SPECIES AND PHYSICAL DATA OF THE MEASURED INSECTS

No.	Species[a]	Mass (mg)	Body length (mm)	Abdomen width (mm)	Azimuth (deg)	Elevation (deg)
1	*Athetis lepigone* (Moschler) #1	21.8	12.5	2	0-90	0-45
2	*Athetis lepigone* (Moschler) #2	28.5	12.5	2	0-90	0-45
3	*Helicoverpa armigera* (Hübner)#1	64.1	16	4	0-90	0-45
4	*Agrotis segetum* (Denis et Schiffermüller) #1	138.1	18	5	0	0-30
5	*Agrotis segetum* (Denis et Schiffermüller) #2	152.3	19	4.5	0-90	0-45
6	*Mythimna separata* (Walker) #1	153.6	19	5	0	0-30
7	*Mythimna separata* (Walker) #2	179	20	5	0	0-30
8	*Agrotis segetum* (Denis et Schiffermüller) #3	188.4	19.5	6	0-90	0-45
9	*Helicoverpa armigera* (Hübner) #2	196.3	18	6	0-90	0-45
10	*Mythimna separata* (Walker) #3	201.7	22.5	6	0	0-30
11	*Mythimna separata* (Walker) #4	229.2	22.5	5.5	0	0-30
12	*Theretra oldenlandiae* (Fabricius) #1	405.7	34	9	0-90	0-45
13	*Theretra oldenlandiae* (Fabricius) #2	474.7	35	8.5	0-90	0-45
14	*Agrius convolvuli* (Linnaeus) #1	770.2	42	10	0-90	0-45
15	*Agrius convolvuli* (Linnaeus) #2	916.6	48.5	11	0-90	0-45

[a]Species: These insects were identified partly by the authors and partly by the researchers of the Chinese Academy of Agricultural Sciences.

measurement error caused by insect trembling, the insect was killed by the essential balm before measurement. The essential balm volatilizes quickly and does not affect the form of the insect. It took about 30 min from the time the insect was killed to the completion of the measurement, so dehydration of the insect would have been negligible.

In our experiment, SMs of 15 insect specimens at azimuths of 0°, 30°, 60°, and 90° and elevations of 0°, 15°, 30°, and 45° were measured (5 of them were only measured at azimuth of 0° and elevations of 0°, 15°, and 30°). The radar frequency was set at 9.4 GHz. The masses of the insect specimens ranged from 21.8 to 916.6 mg and body lengths from 12.5 to 48.5 mm. The species and body-size information is shown in Table I.

Along with the insect, the scattering signals of the empty scene and a metal ball with diameter of 20 mm were measured for the background subtraction and polarization and RCS calibration processing. As the background varies greatly with antenna positions, the empty scenes were measured at every antenna positions. The single target calibration technique was adopted for polarization and RCS calibration [33]. See [32] for more signal processing details about background subtraction and calibration. Note that the measurement setups described in [32] and this article are different because the former does not allow for a change of incident field angle. The concern is that the supporting metal rods may introduce additional clutter and bias the measurement. However, the background subtraction processing can be used to eliminate the effects of the clutter as well as the leakage from the back lobe of the horn antennas. To verify this, the range profiles of metal ball without and after background subtraction at four polarization channels are shown in Fig. 3. The ball was only measured with the azimuth of 0° and elevation of 0° because of its isotropy. Due to the heavy weight, the ball deviated slightly downward from the beam center; thus, the range from ball to the radar is slight less than 2 m. It can be seen that without background subtraction, the target is submerged in clutter and leakage at all four polarization channels. However, after background subtraction, the clutter and leakage have been successfully eliminated, and target at all channels are clearly visible. Thus, the clutter and leakage do not have much influence on the measurement.

TABLE II
TRUE VALUES OF INSECT ORIENTATIONS AT DIFFERENT ANTENNA POSITIONS

Azimuth \ Elevation	0°	15°	30°	45°
0°	90°	90°	90°	90°
30°	120°	121°	124°	129°
60°	150°	151°	153°	158°
90°	0°	0°	0°	0°

The insect orientation is defined as the angle between the projection of body axis on polarization plane and the direction of H-polarization [Fig. 2(a)]. It is ambiguous about 180°. When the elevation is 0°, the orientation varies with the azimuth with the same pace. However, for nonzero elevation, their paces are usually not equal. When the azimuth is 0°, for any antenna position, the insect body axis is always perpendicular to the direction of the H-polarization and coplanar with the V-polarization; thus, the orientation of the insect for this track position is always 90°. When the azimuth is 90°, similarly, the orientation is always 0° at different elevations. The true values of the insect orientation at different antenna positions are listed in Table II.

For ease of understanding, an example for azimuth of 60° is shown in Fig. 4. It can be seen that when elevation is 0°, the orientation is 30°, that is, the sum of the azimuth and the orientation is 90°. When elevation is 90°, the projection of body axis on polarization plane is parallel to H-polarization, where orientation is 0°. For elevations between 0° and 90°, the orientations vary from 30° to 0°.

III. INFLUENCE OF PITCH ANGLE ON RETRIEVAL OF INSECT BIOLOGICAL PARAMETERS

When the azimuth is 0°, the pitch angle is equal to the elevation of the antennas position. Therefore, the insect data measured with azimuth of 0° can be well used to study the influences

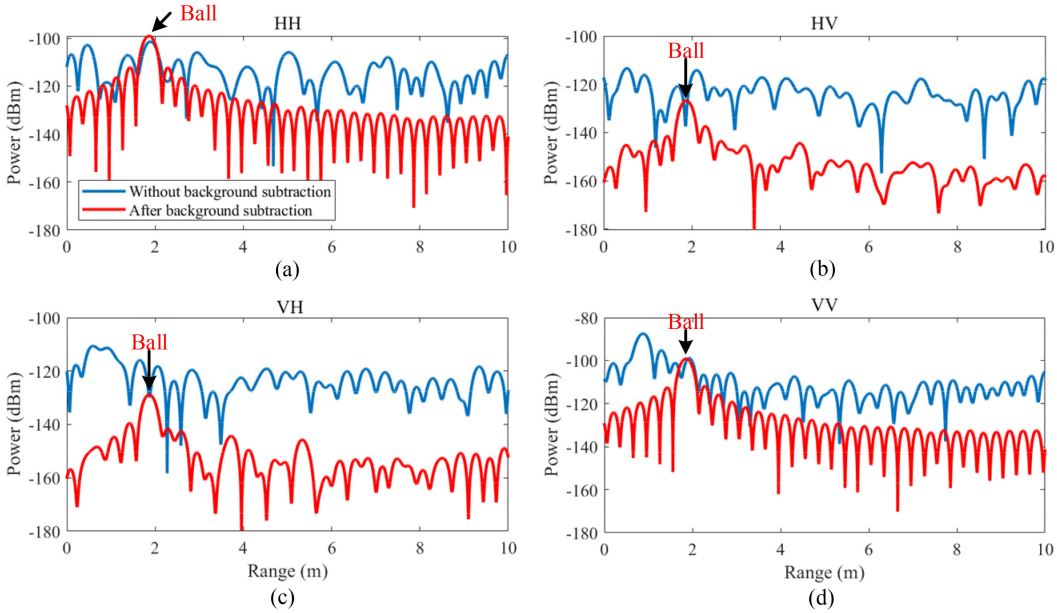

Fig. 3. Range profiles of metal ball without and after background subtraction at polarization channel of (a) HH, (b) HV, (c) VH, and (d) VV.

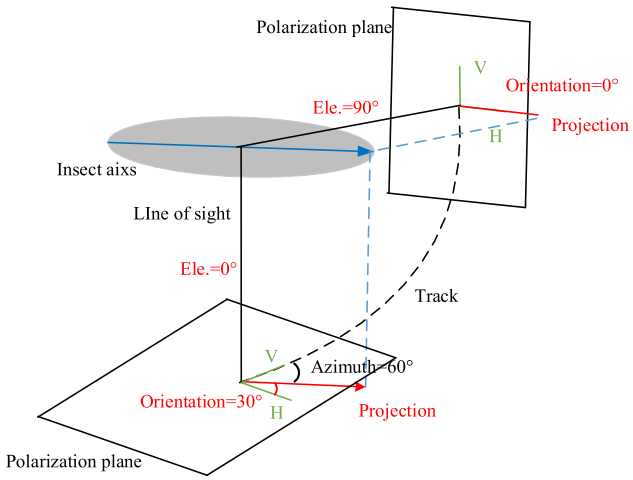

Fig. 4. Diagrammatic sketches of orientations of different elevations.

of pitch angle on the retrieval of insect biological parameters, because in this case, pitch angle is the only variable.

A. Results 1: Influence of Pitch Angle on Orientation Estimation

For a PA insect, the MRD is parallel to the orientation; while for a PE insect, it is perpendicular. Thus, to extract the insect orientation correctly, the insect class (PA or PE) needs to be discriminated. Therefore, to analyze the influence of pitch angle on orientation estimation, both the relationship between the pitch angle and discrimination of the insect class and the relationship between pitch angle and estimation of the MRD should be analyzed.

1) Relationship Between Pitch Angle and Insect Class: The relationship between insect class and pitch angle revealed by the rig measurements is shown in Fig. 5(a), and summarized in Table III. It can be seen that all the insects are PA insects when the pitch angle is 0°. When the pitch angle is 15°, the largest two insects switch from PA to PE insects. As the pitch angle increases further, more insects switch and the mass of the insects making the switch decreases. This means that for large insects, a small pitch angle can cause the class to change, but for a smaller insect, a larger pitch angle is required. Insects with masses less than 180 mg are PA at all pitch angles 0°–45°. Two larger insects exhibit multiple switches as the pitch angle increases: from PA to PE and then back to PA, and in one case back to PE again.

TABLE III
DISCRIMINATION CORRECT RATE AT DIFFERENT PITCH ANGLES

Pitch angles (deg)	Number		Proportion of insects switched to PE	Correct rate ($\Delta\phi$)
	PA insects	PE insects		
0	15	0	0.0%	93.3%
15	13	2	13.3%	100.0%
30	12	3	20.0%	100.0%
45	6	4	40.0%	100.0%

These results indicate that the PA or PE class of insects can depend on the pitch angle and that large insects are more sensitive to pitch angle effects.

According to the definitions of PA and PE insects, the class of an insect depends on the relationship between the RCSs when the polarization direction is parallel and perpendicular to the body axis (hereinafter referred to as “parallel RCS” and “perpendicular RCS”). To explain why the switch happens, the relationships between the pitch angle and the parallel and perpendicular RCSs of three insects with different masses are shown in Fig. 6. For small insect [Fig. 6(a)], both parallel and perpendicular RCSs decrease with the increasing pitch angle, and the parallel RCS is larger than the perpendicular RCS at all

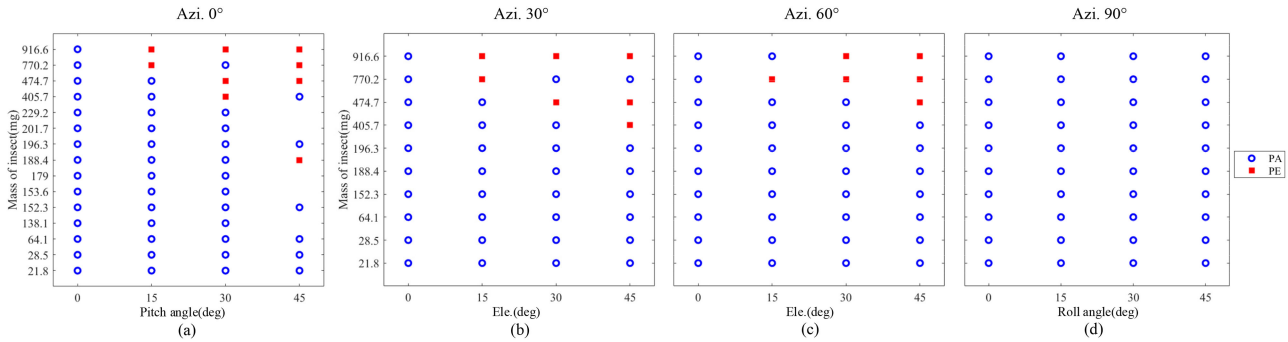

Fig. 5. Relationship between insect class and elevation of 0°, 15°, 30°, and 45° at azimuth of (a) 0°, (b) 30°, (c) 60°, and (d) 90°. At azimuths of 0° and 90°, the elevations are equal to the pitch and roll angle of insects, respectively; thereby, they are written as "pitch angle" and "roll angle" in the figure, respectively. These terms are directly used in the following figures and will not be introduced again.

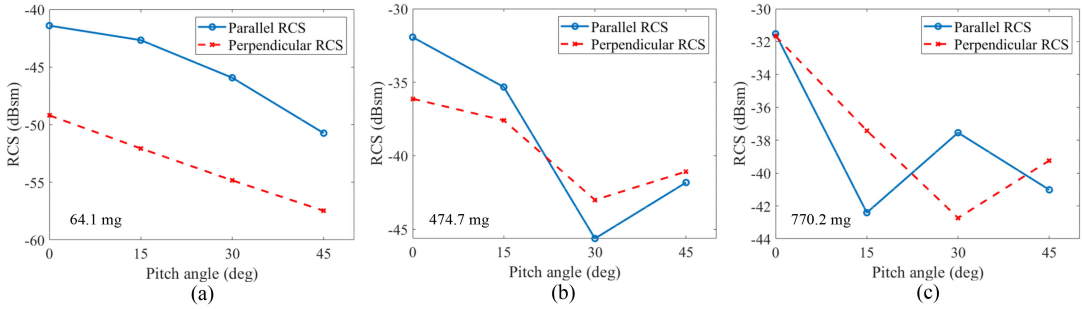

Fig. 6. Relationship between RCSs when polarization direction is parallel and perpendicular to insect body axis for insects with masses of (a) 64.1 mg; (b) 474.7 mg; and (c) 770.2 mg.

pitch angles; thus, the class of the small insect does not change with the pitch angle. With the insect mass increases [Fig. 6(b)], both the parallel and perpendicular RCSs first decrease and then increase with pitch angle. However, the influence of pitch angle on the parallel RCS is greater than that on the perpendicular RCS. This results in the faster reduction of the parallel RCS. When the parallel RCS decreases below the perpendicular RCS at pitch angle of 30°, the class change occurs.

The different influences on two RCSs is reasonable because from the view of radar, the projection of body length (i.e., target dimension in the direction parallel to body axis) decreases with pitch angle, but the projection of body width (i.e., target dimension in the direction perpendicular to body axis) does not vary with pitch angle. With the mass increases further [Fig. 6(c)], the variations of the RCSs become complicated, and the relationship between the two RCSs becomes uncertain; therefore, larger insects exhibit multiple switches as the pitch angle increases.

2) Discrimination of PA and PE Insects: It was reported in [21] that the sign of $\Delta\phi$, the relative phase of the SM eigenvalues, is always negative for parallel insects, and positive for perpendicular insects. Thus, the sign of $\Delta\phi$ can be used to discriminate between the PA and PE classes. The calculation of $\Delta\phi$ is shown in Appendix II-A. However, this method was proposed and verified on the basis that the insect specimens were measured with their body upright and horizontal and the radar was illuminating from directly below. As we analyzed above, the pitch angle can cause the insect class to change. Thus, it is critical to study the relationship between the pitch angle and $\Delta\phi$, and to make clear whether $\Delta\phi$ can be used to discriminate between PA and PE insects when the pitch angle is nonzero.

The relationship between $\Delta\phi$ and the MRD at different pitch angles is shown in Fig. 7(a). As the real orientation of insect is 90° (Table II), an insect with an MRD of about 90° is a PA insect, whose $\Delta\phi$ is expected to be negative, and an insect with an MRD of about 0° is a PE insect, whose $\Delta\phi$ is expected to be positive. If the sign of $\Delta\phi$ does not meet these expectations, a discrimination error will occur and a 90° error in the determined orientation will follow. It can be seen in Fig. 7(a) that when the pitch angle is 0°, all the insect specimens are PA insects. However, the $\Delta\phi$ of one insect is slightly positive, contrary to expectation. When the pitch angle is not 0° (15°, 30°, and 45°), some insects transform from PA to PE, and the signs of the corresponding $\Delta\phi$ also change so that in these cases all the signs of $\Delta\phi$ meet expectation. Thus, only one insect at a pitch angle of 0° is misidentified. The discrimination correct rate for 0° pitch angle is 93.3%, and for nonzero pitch angles are 100%, as shown in Table III. This indicates that the class change can be discriminated by $\Delta\phi$ even when the insect is pitched up at angles as high as 45°.

Four possible reasons can lead to the misidentification. First, due to scattering characteristic of the insect, the true value of $\Delta\phi$ is positive. This is possible because the misidentification method based the sign of $\Delta\phi$ is an empirical method, and some insects may not satisfy this rule as reported in [21]. However,

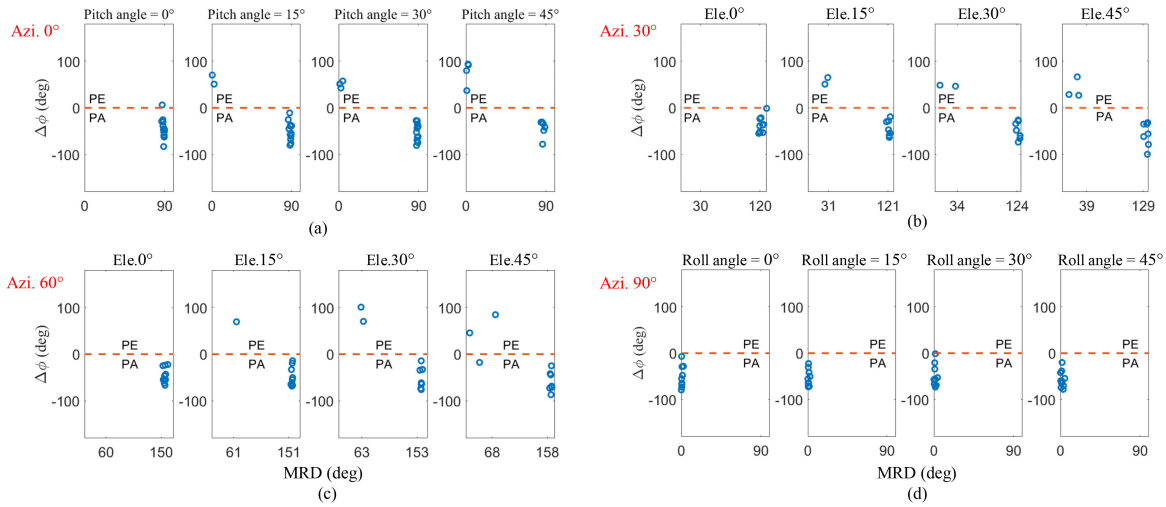

Fig. 7. Relationship between $\Delta\phi$ and MRD at elevations of 0°, 15°, 30°, and 45° at azimuth of (a) 0°, (b) 30°, (c) 60°, and (d) 90°. The red dashed lines indicate the value of 0 rad.

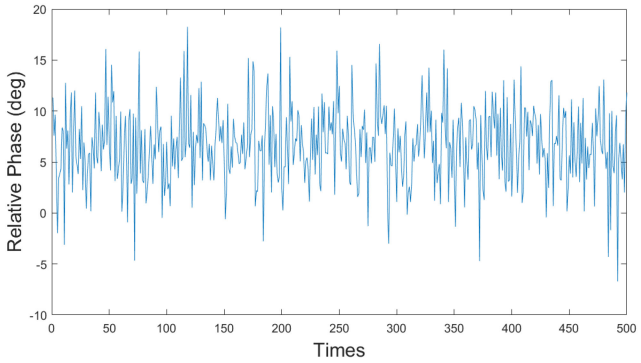

Fig. 8. Simulated $\Delta\phi$ with noise.

as this insect can be well identified at other pitch angles, this is less likely.

The second possible reason is the influence of noise. The misidentified specimen is a small insect with mass of 28.5 mg. The SNRs for HH and VV echo signals are about 28 and 21 dB, respectively. Its $\Delta\phi$ at different pitch angles are 6.3°, −10.9°, −52.1°, and −33.8°, respectively. The $\Delta\phi$ at pitch angle of 0° is close to 0°, and it may change to a positive value due to noise. To support this hypothesis, a Monte Carlo simulation is conducted. The measured HH and VV signals of PSM are set as the true signals of insect, and the complex Gaussian white noise is generated and added to the signals to adjust the SNRs to 28 and 21 dB, respectively. The simulated relative phases are shown in Fig. 8. It can be seen that most relative phases are positive, but some of the relative phases (about 3.2%) switch to negative values due to noise. Therefore, although the probability is not high, the noise does cause the sign change of relative phase.

The third and fourth reasons are errors in the processing of background subtraction and polarization calibration. However, the effects of these two processes are difficult to evaluate because the true value of the insect phase is unknown and the above four reasons are coupled. Nevertheless, as most of the insects can be processed with correct results, we believe that these two processes are reliable.

Above all, the most likely reason for the incorrect result is the noise.

3) Relationship Between Pitch Angle and MRD Error: The estimation accuracy of the MRD determines the accuracy of orientation estimation. The calculation of the MRD is shown in Appendix II-B. The distribution of MRD errors for each of the four pitch angles is shown in Figs. 9(a). It can be seen that MRD errors are mainly less than 2° for the 0° and 15° pitch angles but increase a little for 30° and 45°, though still mostly remaining below 4°. Therefore, when the pitch angle is less than 15°, the influence of the pitch angle on MRD estimation can be neglected; when the pitch angle is larger than 15°, the MRD estimation error will increase, but the impact is limited. The slight increasing MRD with the pitch angle may be caused by the insect legs. The effect of legs on insect RCS was verified through simulation in [34]. The positions of the legs are usually not symmetrical about the body in the experiment, and large components of the legs are not parallel to the body. This indicates that the MRD of legs could not be identical to that of the body, and the legs could affect the MRD of insect. When the pitch angle is 0°, the apparent area illuminated by the incident wave of the body reaches the maximal, and the RCS of the body also reaches the maximal. Thereby, the influence of the legs on MRD is small. With the increase of pitch angle, the apparent area of the body decreases. However, the pitch angle has little influence on the apparent area of the legs (especially those nonparallel components). Thereby, the proportion of RCS contributed by legs increases, and the influence of the legs on MRD could increase with the pitch angle.

B. Results 2: Influence of Pitch Angle on Insect Body Length and Mass Estimation

Currently, the insect body length and mass are estimated based on the assumption that the insect RCS is proportional to the body length or mass at X-band. Based on a large number of

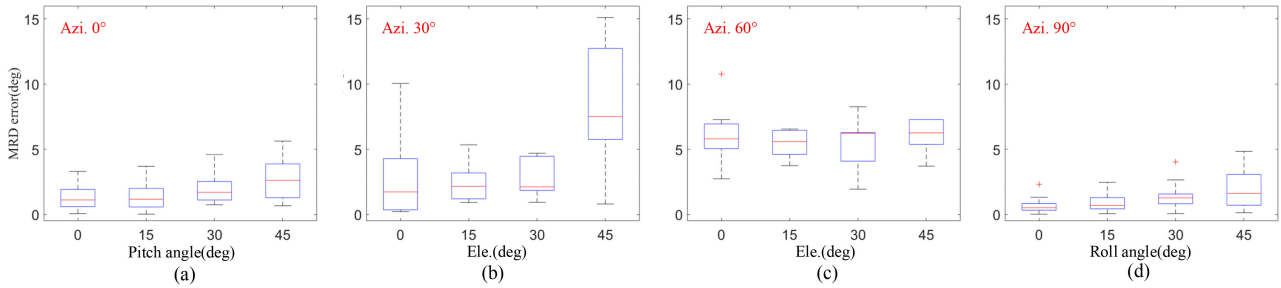

Fig. 9. Relationship between elevation of 0°, 15°, 30°, and 45° and the distribution of MRD errors at azimuth of (a) 0°, (b) 30°, (c) 60°, and (d) 90°.

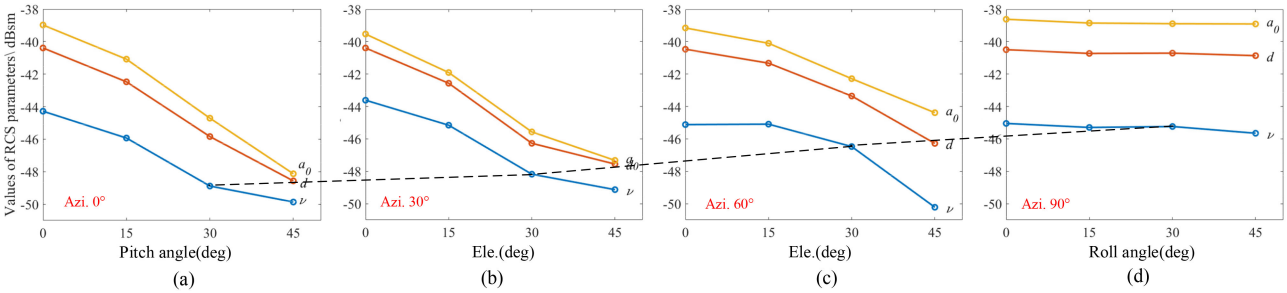

Fig. 10. Relationships between elevation of 0°, 15°, 30°, and 45° and mean RCS parameters at azimuth of (a) 0°, (b) 30°, (c) 60°, and (d) 90°.

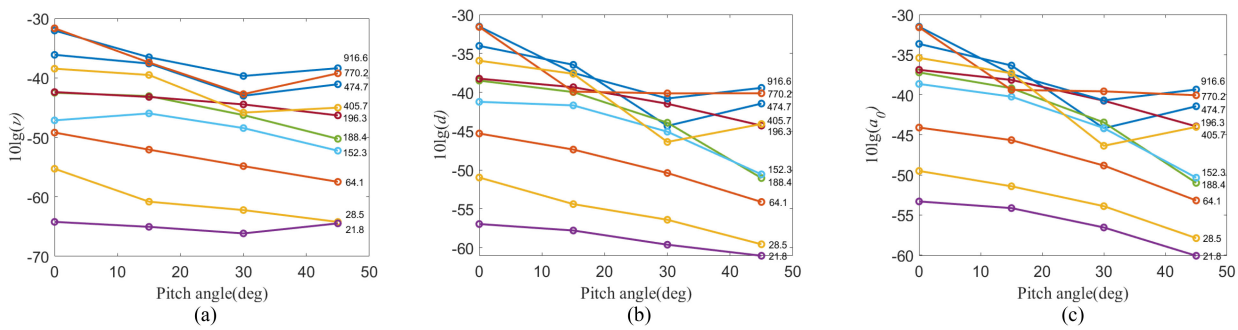

Fig. 11. Relationships between pitch angle and RCS parameters at azimuth of 0° (a) ν; (b) d, and (c) a_0. Each curve represents an insect specimen. The numbers are the masses in mg of the specimens.

measured insect specimens, empirical equations representing the relationships between the RCS and the body length or mass are determined through numerical fitting [20]–[26]. The RCS parameters that can be used to estimate body length and mass include ν, d, a_0, and the parameter pair a_0 and α_2. The calculation of these parameters is shown in Appendix II-C. Radar measurements of insects' RCS are used to estimate body length and mass from empirical formulas. Therefore, in order to study the influence of pitch angle on body length and mass estimation, the relationships between the pitch angle and the RCS parameters should be determined.

1) Relationships Between Pitch Angle and RCS Parameters: The dimensions of ν, d, and a_0 are identical with those of RCS, while α_2 is dimensionless; thus, α_2 will be studied separately from other parameters. The relationships between pitch angle and the mean value of RCS parameters ν, d, and a_0 (over all the specimens) are shown in Fig. 10(a). It can be seen that the means of all three RCS parameters decrease with the increase of pitch angle. The variation range of ν is smaller than that of the other two parameters. The relationships between pitch angle and reductions caused by pitch angle (the difference between the RCS parameter and that at 0° pitch angle) are shown in Table IV. Reductions are around 2 dB at 15° rising to 6–9 dB at 45°.

TABLE IV
RELATIONSHIP BETWEEN PITCH ANGLE AND MEAN REDUCTION OF RCS PARAMETER AT AZIMUTH OF 0°

Pitch angles (deg)	Reductions (relative to 0° pitch angle)		
	ν	d	a_0
0	0	0	0
15	1.65dB	2.08dB	2.1dB
30	4.6dB	5.45dB	5.73dB
45	5.58dB	8.18dB	9.15dB

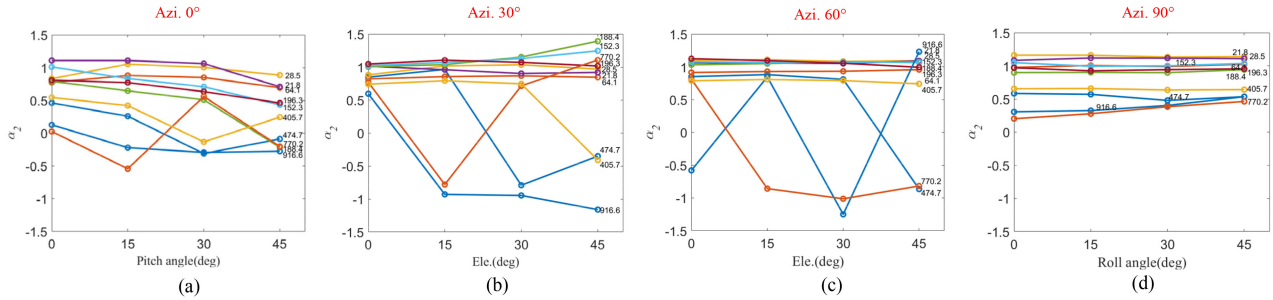

Fig. 12. Relationships between α_2 and elevation of 0°, 15°, 30°, and 45°at azimuth of (a) 0°, (b) 30°, (c) 60°, and (d) 90°.

TABLE V
EMPIRICAL EQUATIONS FOR INSECT BODY LENGTH AND MASS ESTIMATION

	Parameters	Empirical equations [20]
Bdoy length (mm)	ν	$L=1.0500\cdot\left[\lg(\upsilon)\right]^3+19.4611\cdot\left[\lg(\upsilon)\right]^2+121.9888\cdot\left[\lg(\upsilon)\right]+270.7600,\ \lg(\upsilon)\in(-8.23,-2.48)$
	d	$L=2.2489\cdot\left[\lg(d)\right]^3+39.0919\cdot\left[\lg(d)\right]^2+225.9922\cdot\left[\lg(d)\right]+445.8781,\ \lg(d)\in(-7.73,-2.8)$
Mass (mg)	ν	$\lg M=0.0118\cdot\left[\lg(\upsilon)\right]^3+0.2117\cdot\left[\lg(\upsilon)\right]^2+1.7519\cdot\left[\lg(\upsilon)\right]+6.9831,\ \lg(\upsilon)\in(-8.23,-2.48)$
	d	$\lg M=0.0412\cdot\left[\lg(d)\right]^3+0.7184\cdot\left[\lg(d)\right]^2+4.6193\left[\lg(d)\right]+12.0370,\ \lg(d)\in(-7.73,-2.8)$
	a_0	$\lg M=2.3457+0.8947\lg a_0+0.2566(\lg a_0)^2+0.0482(\lg a_0)^3,\ \lg a_0\in(-3.54,1.23)$
	a_0 & α_2	$\lg M=2.6695+0.6841\cdot\lg(a_0)$-$0.3768\alpha_2$+$0.0417\cdot\left[\lg(a_0)\right]^2,\ \lg a_0\in(-3.54,1.23)$

The relationships between pitch angle and RCS parameters for each insect specimen are shown in Fig. 11. For most insects, the RCS parameters decrease with increasing pitch angle, which is caused by the decrease of the apparent area illuminated by the incident wave with the pitch angle. However, for insects with masses larger than about 400 mg, this trend reverses above a pitch angle of 30°. This reversal occurs in all three RCS parameters (Fig. 11). This is because the larger insects may be larger than the first resonance and fall within the resonance as the apparent area becomes "smaller" due to the pitch angle.

The relationships between the pitch angle and α_2 for each insect specimen are shown in Fig. 12(a). For most of the insects, there is a slight decrease of α_2 with increasing pitch angle. However, as with the other RCS parameters, the variation of α_2 for the larger insects is more complicated. For example, for the insect with a mass of 770.2 mg, α_2 has a sudden increase between the pitch angles of 15° and 30°. For the insects with masses of 405.7 and 474.7 mg, α_2 decreases with pitch angle when pitch angle is less than 30°, and increases when pitch angle is 45°.

2) Relationships Between Pitch Angle and Estimation Errors of Insect Body Length and Mass: The reduction of RCS parameters caused by the pitch angle would lead to the body length and mass being underestimated if the empirical formulas estimated previously from measurements at 0° pitch angle were used. Here, we will quantitatively analyze the influence of pitch angle on body length and mass estimation.

The empirical equations for insect body length and mass estimation based on the RCS parameters ν, d, a_0, and parameter pair a_0 and α_2 published in [20] are listed in Table V. All four parameters are used for mass estimation, but for body length only equations involving ν and d have been developed. For each insect specimen, the estimated body length or mass at 0° pitch angle is set as a reference value, and the difference between the estimated value at nonzero pitch angle and the reference value is the error introduced by the pitch angle. The relative error of body length and mass estimation caused by the nonzero pitch angle is defined as

$$\text{Relative error}=\frac{\text{Estimated value}-\text{Reference value}}{\text{Reference value}}\times 100\%. \tag{1}$$

The mean value of the relative errors (MRE) over all insect specimens is used to quantify the effect of pitch angle on the body length and mass estimation.

For body length estimation, the MREs for the ν and d equations are listed in Table VI. For both ν and d methods, the estimated body length decreases with increasing pitch angle. The sign "–" of the MRE indicates that the measured value is smaller than the true value. MREs are –7.2% for ν and –13.5% for d at 15° rising to –23.5% and –37.5% at 45°. Obviously, the influence of pitch angle on the d method is greater than that on the ν method.

For mass estimation, the MREs of the four methods are also listed in Table VI. The influence of pitch angle on mass estimation is greater than that on body-length estimation. Among the four methods, the ν method is the least affected by the pitch angle, and the a_0 and α_2 method the most affected. The influence

TABLE VI
RELATIONSHIP BETWEEN PITCH ANGLE AND RELATIVE ERRORS OF BODY LENGTH AND MASS ESTIMATION AT AZIMUTH OF 0°

Pitch angles	Relative error (relative to 0° pitch angle)					
	Body length		Mass			
	ν	d	ν	d	a_0	a_0 & α_2
0°	0.0%	0.0%	0.0%	0.0%	0.0%	0.0%
15°	–7.2%	–13.5%	–17.7 %	–28.4 %	–32.2 %	–36.9 %
30°	–19.3%	–31.3%	–42.1 %	–57.0 %	–62.6 %	–119.6 %
45°	–23.5%	–37.5%	–52.3 %	–72.3 %	–77.6 %	–368.7 %

of pitch angle on the a_0 and α_2 method is much greater than that of the other three methods. This is because both a_0 and α_2 are affected by the pitch angle, and pitch angle may cause a change of the sign of α_2, which leads to a large estimation error.

IV. INFLUENCE OF ROLL ANGLE ON RETRIEVAL OF INSECT BIOLOGICAL PARAMETERS

When the azimuth is 90°, the roll angle is equal to the elevation of the antennas position. The insect data measured with azimuth of 90° are used to study the influences of roll angle on the retrieval of insect biological parameters as roll angle is the only variable.

A. Influence of Roll Angle on Orientation Estimation

The relationship between the insect class and the roll angle is shown in Fig. 5(d). All insects at all roll angles are PA insects. This indicates that the increasing of roll angle does not lead to the change of insect class.

The relationship between $\Delta\phi$ and the MRD at different roll angles is shown in Fig. 7(d). When the azimuth is 90°, the insect orientation is 0° at all roll angles (Table II). In this case, the orientation of 0° indicates the insect is a PA insect, and the expected sign of $\Delta\phi$ is negative. We can see that all the insects are PA insects and all the corresponding $\Delta\phi$ are below the dashed lines of zero, which means all the insects can be correctly discriminated with the sign of $\Delta\phi$. This reveals that the roll angle has little influence on the discrimination of the insect class.

Fig. 9(d) shows the relationship between the distribution of MRD errors for each roll angle. The MRD error increases slightly with the increasing of roll angle. The MRD errors are mainly less than 1° at 0° rising to 3° at 45°. Compared with Fig. 9(a), the influence of roll angle is less than that of pitch angle. This slight increase of MRD error may be caused by the asymmetry of the insect body structure when viewed from the side (especially the insect legs), and this asymmetry increases with the roll angle increases.

B. Influence of Pitch Angle on Insect Body Length and Mass Estimation

The relationships between the roll angle and the RCS parameters ν, d, and a_0 are given in Fig. 10(d). It can be seen that the RCS parameters hardly vary with roll angle. All the reductions are less than 0.61 dB (Table VII). The relationships between

TABLE VII
RELATIONSHIP BETWEEN ROLL ANGLE AND MEAN REDUCTION OF RCS PARAMETER AT AZIMUTH OF 90°

Roll angles (deg)	Reductions (relative to 0° pitch angle)		
	ν	d	a_0
0	0	0	0
15	0.25dB	0.23dB	0.23dB
30	0.19dB	0.21dB	0.27dB
45	0.61dB	0.37dB	0.29dB

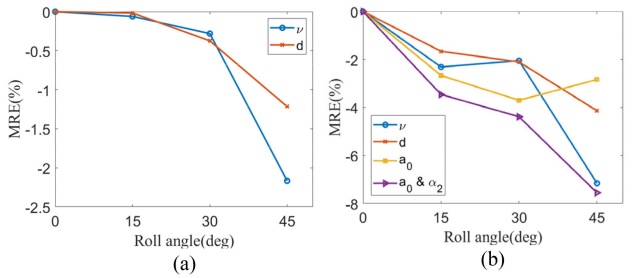

Fig. 13. Relationship between roll angle and relative errors of (a) body length and (b) mass estimation at azimuth of 0°.

the roll angle and α_2 for each insect specimen are shown in Fig. 12(d). For most of the insects, α_2 hardly varies with the increasing roll angle. However, α_2 of the two largest insects slightly increase with the roll angle.

The influences of the roll angle on the body length and mass estimations are shown in Fig. 13. The MREs of body length estimation slightly increase with the increasing roll angle. The MREs are less than -0.3% at roll angles less than 30° rising to less than -2.2% at 45°. The influences of roll angle on mass estimations are slightly larger. The MREs range from -1% to -4% for the a_0 and d methods, and -2% to -8% for the ν and a_0 and α_2 methods. Not surprisingly, the a_0 and α_2 method is most affected by roll angle. Compared with pitch angle, the influence of roll angle is slight.

V. INFLUENCE OF THE COMBINATION OF PITCH AND ROLL ANGLE ON RETRIEVAL OF INSECT BIOLOGICAL PARAMETERS

In the above two sections, the influences of pitch and roll angles on the retrieval of insect biological parameters are discussed, respectively. In this section, the more general case when both pitch and roll angles are nonzero is considered. The additional measured SMs of 10 insect specimens at azimuths of 30° and 60° are used. The real pitch and roll angles at different

TABLE VIII
TRUE VALUES OF PITCH ANGLES AT DIFFERENT ANTENNA POSITIONS

Azimuth \ Elevation	0°	15°	30°	45°
0°	0°	15°	30°	45°
30°	0°	13°	26°	38°
60°	0°	7°	14°	21°
90°	0°	0°	0°	0°

TABLE IX
TRUE VALUES OF ROLL ANGLES AT DIFFERENT ANTENNA POSITIONS

Azimuth \ Elevation	0°	15°	30°	45°
0°	0°	0°	0°	0°
30°	0°	8°	16°	27°
60°	0°	13°	27°	41°
90°	0°	15°	30°	45°

combinations of azimuth and elevation are shown in Tables VIII and IX, respectively. It can be seen that for each nonzero elevation, the component of pitch angle decreases with azimuth, while that of roll angle increases with azimuth.

A. Influence on Orientation Estimation

1) Insect Class: The insect classes at different combinations of elevation and azimuth are shown in Fig. 5. With the increasing of azimuth, the mass of the insects making the switch increases. This indicates that the influence of different combinations of azimuth and elevation on insect class decreases with azimuth. This decrease trend is similar to that of pitch angle component (Table VIII), but different with that of roll angle component (Table IX). If the conclusions drawn in the previous two sections (i.e., pitch angle causes class change of insect, while roll angle has little influence on class change) are utilized to explain this phenomenon, this result makes sense. That is, the class change of insect is mainly caused by the pitch angle component, and the roll angle component has little influence on class change. With the increasing azimuth, the pitch angle component decreases, which causes the decreasing influence on class change. This conclusion can be also supported by a special case: as seen in Tables VIII and IX, for the combinations of (Azi. $= 0°$ and Ele. $= 15°$), (30°, 15°), and (60°, 30°), the values of pitch angle are close, but the roll angles are different. The mass of the insects making the class switch at these combinations are identical. Therefore, the effects of pitch and roll angles on insect classes can be decoupled.

2) Discrimination of PA and PE Insects: Relationships between $\Delta\phi$ and MRD at azimuths of 30° and 60° are shown in Figs. 7(b) and (c), respectively. For azimuths of 30° and 60°, the true values of insect orientations (Table II) range from 120° to 129° and 150° to 158°, respectively. Thus, the insects with MRD of 30°–39° and 60°–68° are PE insects, respectively, and others are PA insects. It can be seen that only one PE insect at azimuth of 60° and elevation of 45° has an unexpected negative $\Delta\phi$. $\Delta\phi$ of the rest PE insects are positive, and $\Delta\phi$ of all PA insects are negative, which are expected. Thus, when pitch and roll angles are both nonzero, they have no obvious influence on the discrimination of PA and PE insect. This conclusion is the generalization of the conclusions obtained in the previous two sections when only the pitch angle or the roll angle is variable. Therefore, the PE and PA discrimination method based on $\Delta\phi$ can be well used to the insect with general pitch and roll angles combinations. That is, the insect flying gesture has little influence on the discrimination method.

3) MRD Error: The distribution of MRD estimation errors at different azimuths are shown in Fig. 9. As analyzed in the previous two sections, MRD errors slightly increase with both pitch and roll angles [Fig. 9(a) and (d)]. At azimuths of 30° and 60°, both pitch and roll angles increase with elevation (Tables VIII and IX); however, the MRD errors do not increase significantly with elevation as expected. The overall MRD errors at azimuth of 30° and 60° are larger than that at azimuth of 0° and 90°, but no obvious relationship with pitch and roll angles can be found with general pitch and roll angles combinations.

A previous study of our team revealed that the influence of a determined level of polarization errors (amplitude and phase imbalance between H- and V-polarization channels) on the estimation error of MRD varies with the true value of insect MRD [35]. Specifically, the minimal estimation error occurs when the true MRD is 0° or 90°, while the maximum occurs at MRD of about 45°. This article is based on the horizontal flight hypothesis. For this article, when the elevation is 0° at each azimuth, both pitch and roll angles are zero, and the measurement scene degenerates into the horizontal flight of insects. It can be seen in Fig. 9 that the variation law of MRD errors with azimuth (i.e., true value of MRD) for horizontal flight is consistent with the conclusion in [35]. In addition, there is no evident difference between the MRD errors for nonzero elevations (nonhorizontal flight) and zero elevation (horizontal flight) except the case that azimuth is 30° and elevation is 45°. Therefore, it is reasonable to believe that the influence of the residual polarization errors on MRD estimation masks that of pitch and roll angles. The difference between the special case (Azi. $= 30°$ and Ele. $= 45°$) and the case (60° and 45°) is that the pitch angle of the former is larger (pitch $= 38°$ and roll $= 27°$), and the roll angle of the latter is larger (pitch $= 21°$ and roll $= 41°$). The larger MRD errors of the special case indicates that the influence of pitch angle on MRD error is larger than that of roll angle. When the pitch angle is large (e.g., 38°), effect of pitch angle combining that of residual polarization errors emerge and may cause large MRD errors.

B. Influence on RCS Parameters

As the influence of combinations on body length and mass estimation arises from its influence on RCS parameters, the influences of general combinations of pitch and roll angles on RCS parameters are now presented.

The relationships between RCS parameters and different combinations of pitch and roll angles are shown in Figs. 10(b) and (c). As analyzed in the previous two sections, pitch angle causes the decrease of RCS parameters [Fig. 10(a)], while roll angle has little influence on RCS parameters [Fig. 10(d)]. For azimuth of 30° and 60°, the pitch angle component increases with elevation (row in Table VIII), and the RCS parameters decrease with the

increasing pitch angle component as expected [Figs. 10(b) and (c)]. This result is similar to that when the pitch angle is the only variable [Fig. 10(a)].

For each elevation (except 0°), the pitch angle component decreases with the increasing azimuth (column in Table VIII). Thus, its influence on RCS parameters (compared with the influence at azimuth of 0°) should decrease with the increasing azimuth at each elevation. As one of the examples, the relationship between ν and azimuth at elevation of 30° is shown as the black dashed line in Fig. 10. As the scales of the longitudinal axis of the four figures in Fig. 10 are identical, the trend of the dashed line with azimuth reflects the degree of the influence. A higher value of ν represents the difference between this value and the value when both pitch and roll angles are zero is smaller, that is, the influence is less. It can be seen that the dashed line increases with the azimuth; thus, the influence on ν decreases with azimuth, which is expected. Fig. 10 shows that most cases meet this law. However, some of the values are slightly lower than expected, such as ν at azimuth of 60° and elevation of 30° and a_0 at azimuth of 30° and elevation of 30°. All the deviation values are less than 1 dBsm. These unexpected values may be caused by the normal amplitude fluctuation in measurement.

The relationships between α_2 and general combinations of pitch and roll angles are shown in Figs. 12(b) and (c). At the azimuth of 30° and 60°, α_2 of the small insects varies little with elevation and their distribution is more concentrated, while the variation of α_2 for large insects is more complicated. At azimuth of 90°, α_2 of the large and small insects have the similar variation. It can be seen that the complicated variations of α_2 for large insects occur at Azimuth of 0°, 30°, and 60°, where the pitch angle component is not zero. This indicates that the pitch angle component has greater influence on α_2 of the large insects, and both pitch and roll angles have little influence on α_2 of the small insects. The influence of pitch angle component on α_2 of the large insects mainly comes from the insect class switch caused by it, which leads to the sign change of α_2.

VI. Conclusion

In this article, the SMs of 15 insects at different pitch and roll angles, measured with a multiaspect coherent fully polarimetric rig, are presented. The influence of the pitch angle only, roll angle only, and a general combination of pitch and roll angles on insect class and its discrimination, orientation estimation, RCS parameters measurement, and body length and mass estimation have been analyzed.

It was found that the pitch angle can cause class switching, and large insects are more sensitive to pitch angle in this respect. However, this class change can be discriminated by the relative phase $\Delta\phi$ of the SM, and the pitch angle then has little influence on the class discrimination. As the insect class depends on the relationship between the parallel and perpendicular RCSs, the class switch is mainly caused by the difference influences of pitch angle on the parallel and perpendicular RCSs.

The pitch angle can cause an error in estimates of orientation, but this is small (mainly $<4°$); it may arise from minor asymmetries in the insect's body form. The RCS parameters decrease as the pitch angle increases; among these parameters, ν is the least affected by pitch angle. The mean reductions of ν at pitch angles of 15°, 30°, and 45° are 1.65, 4.6, and 5.58 dB, respectively. The decrease of RCS parameters results in large errors in estimates of body lengths and masses. Among these body length and mass estimation methods, the ν method is the least affected by the pitch angle. Nevertheless, for the ν method, the MREs of body length estimation caused by pitch angle at pitch angles of 15°, 30°, and 45° are -7.2%, -19.3%, and -23.5%, respectively, and for mass estimation, the MREs are -17.7%, -42.1%, and -52.3%, respectively.

The roll angle has little influence on the class discrimination, MRD estimation, RCS parameters, and body length estimation, and slightly affects the accuracy of the mass estimation. Compared with the pitch angle, the influence of the roll angle is insignificant. This is because the insect body is approximately an ellipsoid. The change of roll angle is equivalent to rotating the ellipsoid around the long axis. In this process, the geometric structure of insects relative to radar changes little, and only the position of insect legs and wings changes, which causes the little influence on the retrieval of biological parameters.

When both pitch and roll angles are nonzero, the influence of the combinations of pitch and roll angles can be decoupled. That is, the final influence is approximately the linear superposition of the influence of pitch angle and roll angle.

Three-dimensional (3-D) RCS of an insect for a certain polarization is determined, and it varies with polarization. In the traditional measurement case that the insects maintain a horizontal flight attitude and radar looks vertically, only ventral aspect of 3-D RCS is measured. In this article, through varies the azimuth and elevation of antenna positions (pitch and roll angles of insect), more aspects of 3-D RCS are analyzed. It is found that the variation of 3-D RCS of large insects with aspect is more complicated than that of small insects. The fluctuation of 3-D RCS with aspect is part of a particular insect size RCS signature. The complicated and different variation of 3-D parallel RCS and 3-D perpendicular RCS with aspect lead to the translocation of their size relationship, and the translocation causes the switch of insect class. Luckily, most of class change caused by the 3-D RCS signature can be discriminated by the relative phase $\Delta\phi$ of the SM. Misidentifications only occur at two aspects in the measurement, and these may be caused by the noise or just the signature for a few aspects for particular insect sizes.

In this article, only 15 insect specimens were measured, which are not enough to give a very accurate conclusion about the influence of pitch angle on measurement of insect biological parameters, and even less so for estimation of body length and mass. However, the insect specimens extended in mass from 21.8 to 916.6 mg. Thus, the qualitative conclusion in this article is reliable. In addition, in this article, only pitch angles of 0°, 15°, 30°, and 45° are considered. For many flying insects, the pitch angle may be small; thus, more details of the influence of pitch angles between 0° and 15° are desirable. To obtain more accurate quantitative conclusions, more insect specimens of different body sizes measured at more pitch angles are required in the future.

It is shown in our article that the pitch angle causes large errors in insect body length and mass estimation, and these are caused by the decrease of the RCS parameters with increasing pitch angle. To deduce the estimation errors, the empirical equations of the body length and mass estimation could be refitted at different pitch angles, respectively. This would require a large number of insect specimens measured under different pitch angles. In addition, if these empirical equations are applied to the operational environment, a method to estimate the pitch and roll angles of the flying insect from the radar measurement is required. This is an appropriate topic for future investigations.

For the insects observed with currently operating vertical-looking entomological radars, the pitch angle is generally assumed to be small and the body upright (i.e., roll angle 0°). If these assumptions are correct, the influence of small pitch angle on insect biological parameters estimation may be slight. However, for a tracking radar, the antenna beam always follows the target rather than striking it from below. The pitch and roll angles may be large, and the insect body may not be upright (relative to the radar beam). Thus, for a tracking radar, both the pitch angle and the roll angle of the insect's body need to be considered.

APPENDIX I
ABBREVIATIONS

No.	Abbreviations	Definitions
1	Azi.	Azimuth
2	Ele.	Elevation
3	H	Horizontal
4	IMR	Insect Monitoring Radar
5	MRD	Maximum RCS direction
6	MRE	Mean value of the relative error
7	PA	Parallel
8	PE	Perpendicular
9	PPI	Plan position indicator
10	RCS	Radar cross-section
11	SM	Scattering matrix
12	SNR	Signal-to-noise
13	STCT	Single target calibration technique
14	3D	Three-dimensional
15	V	Vertical
16	VLR	Vertical-Looking Radar
17	ZLC	Zenith-pointing Linear-polarized Conical scan

APPENDIX II
PARAMETERS CALCULATION BASED ON SM

Suppose the SM of the insect is written as

$$\mathbf{S} = \begin{bmatrix} s_{11} & s_{12}e^{j\beta} \\ s_{21}e^{j\beta'} & s_{22}e^{j\gamma} \end{bmatrix} \tag{2}$$

where s_{11}, s_{12}, s_{21}, and s_{22} represent the amplitude of each element, respectively; and β, β', and γ represent the phases.

A. Relative Phase $\Delta\phi$[21]

The two eigenvalues of the insect SM can be written as

$$\mu_1 = \frac{1}{2}\left(s_{11}+s_{22}e^{j\gamma}\right)+\frac{1}{2}\sqrt{\left(s_{11}-s_{22}e^{j\gamma}\right)^2+4s_{12}s_{21}e^{j(\beta+\beta')}} = |\mu_1|\,e^{j\phi_1} \tag{3}$$

$$\mu_2 = \frac{1}{2}\left(s_{11}+s_{22}e^{j\gamma}\right)-\frac{1}{2}\sqrt{\left(s_{11}-s_{22}e^{j\gamma}\right)^2+4s_{12}s_{21}e^{j(\beta+\beta')}} = |\mu_2|\,e^{j\phi_2} \tag{4}$$

where $|\mu_1|$ and $|\mu_2|$ represent the amplitudes of μ_1 and μ_2, respectively, and $|\mu_1| \geq |\mu_2|$; ϕ_1 and ϕ_2 represent the phases.

$\Delta\phi$ is defined as

$$\Delta\phi = \phi_1 - \phi_2 + 2k\pi, k = 0, \pm 1 \tag{5}$$

where ϕ_1 and $\phi_2 \in (-\pi, \pi]$, and $2k\pi$ is introduced in order to make $\Delta\phi \in (-\pi, \pi]$.

$\Delta\phi$ can also be calculated by

$$\Delta\phi = \arg\left(\frac{\mu_1}{\mu_2}\right) \tag{6}$$

where $\arg(\cdot)$ represents phase taking operation. Equation (6) avoids the judgment of k value.

B. MRD [19], [20]

MRD can be written as

$$\alpha_m = \begin{cases} \arctan\left[\dfrac{\mathrm{Re}\left(\frac{1}{\sqrt{1+\kappa^2}}\right)}{\mathrm{Re}\left(\frac{\kappa}{\sqrt{1+\kappa^2}}\right)}\right] & \mu_1 - s_{11} \neq 0 \\ 0^\circ & \mu_1 - s_{11} = 0 \end{cases} \tag{7}$$

where

$$\kappa = \frac{s_{12}}{\mu_1 - s_{11}}. \tag{8}$$

C. RCS Parameters [20]

ν and d can be represented as

$$\nu = \begin{cases} \lambda_2 & \Delta\phi < 0 \\ \lambda_1 & \Delta\phi > 0 \end{cases} \tag{9}$$

$$d = \sqrt{\lambda_1\lambda_2} \tag{10}$$

where

$$\lambda_1 = \frac{(g_{11}+g_{22})+\sqrt{(g_{11}-g_{22})^2+4g_{12}g_{21}}}{2} \tag{11}$$

$$\lambda_2 = \frac{(g_{11}+g_{22})-\sqrt{(g_{11}-g_{22})^2+4g_{12}g_{21}}}{2} \tag{12}$$

and

$$\begin{cases} g_{11} = s_{11}^2 + s_{12}^2 \\ g_{12} = s_{11}s_{12}e^{j\beta} + s_{12}s_{22}e^{j(\gamma-\beta)} \\ g_{21} = s_{11}s_{12}e^{-j\beta} + s_{12}s_{22}e^{-j(\gamma-\beta)} \\ g_{22} = s_{12}^2 + s_{22}^2. \end{cases} \tag{13}$$

a_0 and α_2 can be written as

$$a_0 = \frac{1}{8}\left(3s_{11}^2 + 3s_{22}^2 + 4s_{12}^2 + 2s_{11}s_{22}\cos\gamma\right) \tag{14}$$

$$\alpha_2 = \begin{cases} \frac{\sqrt{a_{11}^2+a_{12}^2}}{a_0} & \Delta\phi < 0 \\ -\frac{\sqrt{a_{11}^2+a_{12}^2}}{a_0} & \Delta\phi > 0 \end{cases} \tag{15}$$

where

$$\begin{cases} a_{11} = \frac{1}{2}\left(s_{11}^2 - s_{22}^2\right) \\ a_{12} = s_{12}\left[s_{11}\cos\beta + s_{22}\cos\left(\beta - \gamma\right)\right]. \end{cases} \tag{16}$$

ACKNOWLEDGMENT

The authors are grateful to V. Alistair Drake who edited the paper for better English, and made many insightful comments and good suggestions.

REFERENCES

[1] S. Bauer and J. H. Bethany, "Migratory animals couple biodiversity and ecosystem functioning worldwide," *Science*, vol. 344, no. 6179, 2014, Art. no. 1242552.
[2] G. Hu *et al.*, "Mass seasonal bioflows of high-flying insect migrants," *Science*, vol. 354, no. 6319, pp. 1584–1587, 2016.
[3] R. A. Holland, W. Martin, and S. W. David, "How and why do insects migrate?," *Science*, vol. 313, no. 5788, pp. 794–796, 2006.
[4] J. W. Chapman *et al.*, "Flight orientation behaviors promote optimal migration trajectories in high-flying insects," *Science*, vol. 327, no. 5966, pp. 682–685, 2010.
[5] R. Buderi, *The Invention That Changed the World: How a small Group of Radar Pioneers Won the Second World War and Launched a Technological Revolution*. New York, NY, USA: Simon and Schuster, 1996.
[6] A. B. Crawford, "Radar reflections in the lower atmosphere," *Proc. IRE*, vol. 37, pp. 404–405, 1949.
[7] R. Hajovsky, A. Deam, and A. LaGrone, "Radar reflections from insects in the lower atmosphere," *IEEE Trans. Antennas Propag.*, vol. 14, no. 2, pp. 224–227, Mar. 1966.
[8] G. W. Schaefer, "Radar observations of insect flight," in *Proc. Symposia Roy. Entomol. Soc. London*, 1976, pp. 157–195.
[9] V. A. Drake, "Quantitative observation and analysis procedures for a manually operated entomological radar," CSIRO, Melbourne, VIC, Australia, Rep. 19, 1981.
[10] V. A. Drake and D. R. Reynolds, *Radar Entomology: Observing Insect Flight and Migration*. Wallingford, U.K.: CABI, 2012.
[11] T. Long *et al.*, "Entomological radar overview: System and signal processing," *IEEE Aerosp. Electron. Syst. Mag.*, vol. 35, no. 1, pp. 20–32, Jan. 2020.
[12] K. Cui, C. Hu, R. Wang, Y. Sui, H. Mao, and H. Li, "Deep-learning-based extraction of the animal migration patterns from weather radar images," *Sci. China Inf. Sci.*, vol. 63, no. 4, 2020, Art. no. 140304.
[13] C. Hu, K. Cui, R. Wang, T. Long, S. Ma, and K. Wu, "A retrieval method of vertical profiles of reflectivity for migratory animals using weather radar," *IEEE Trans. Geosci. Remote Sens.*, vol. 58, no. 2, pp. 1030–1040, Feb. 2020.
[14] R. Wang, T. Zhang, C. Hu, J. Cai, and W. Li, "Digital detection and tracking of tiny migratory insects using vertical-looking radar and ascent and descent rate observation," *IEEE Trans. Geosci. Remote Sens.*, vol. 60, 2022, Art. no. 5101615, doi: 10.1109/TGRS.2021.3071934.
[15] J. W. Chapman, V. A. Drake, and D. R. Reynolds, "Recent insights from radar studies of insect flight," *Ann. Rev. Entomol.*, vol. 56, pp. 337–356, 2011.
[16] J. W. Chapman, D. R. Reynolds, and A. D. Smith, "Vertical-looking radar: A new tool for monitoring high-altitude insect migration," *BioScience*, vol. 53, no. 5, pp. 503–511, 2003.
[17] V. A. Drake, S. Hatty, C. Symons, and H. Wang, "Insect monitoring radar: Maximizing performance and utility," *Remote Sens.*, vol. 12, no. 4, 2020, Art. no. 596.
[18] C. Hu, W. Li, R. Wang, Y. Li, W. Li, and T. Zhang, "Insect flight speed estimation analysis based on a full-polarization radar," *Sci. China Inf. Sci.*, vol. 61, no. 10, 2018, Art. no. 109306.
[19] C. Hu, W. Li, R. Wang, C. Liu, T. Zhang, and W. Li, "Accurate insect orientation extraction based on polarization scattering matrix estimation," *IEEE Geosci. Remote Sens. Lett.*, vol. 14, no. 10, pp. 1755–1759, Oct. 2017.
[20] C. Hu, W. Li, R. Wang, T. Long, C. Liu, and V. A. Drake, "Insect biological parameter estimation based on the invariant target parameters of the scattering matrix," *IEEE Trans. Geosci. Remote Sens.*, vol. 57, no. 8, pp. 6212–6225, Aug. 2019.
[21] C. Hu, W. Li, R. Wang, T. Long, and V. A. Drake, "Discrimination of parallel and perpendicular insects based on relative phase of scattering matrix eigenvalues," *IEEE Trans. Geosci. Remote Sens.*, vol. 58, no. 6, pp. 3927–3940, Jun. 2020.
[22] W. Li, C. Hu, R. Wang, S. Kong, and F. Zhang, "Comprehensive analysis of polarimetric radar cross-section parameters for insect body width and length estimation," *Sci. China Inf. Sci.*, vol. 64, no. 2, 2021, Art. no. 122302.
[23] R. Wang *et al.*, "Migratory insect multifrequency radar cross sections for morphological parameter estimation," *IEEE Trans. Geosci. Remote Sens.*, vol. 57, no. 6, pp. 3450–3461, Jun. 2019.
[24] C. Hu, S. Kong, R. Wang, and F. Zhang, "Radar measurements of morphological parameters and species identification analysis of migratory insects," *Remote Sens.*, vol. 11, no. 17, 2019, Art. no. 1977.
[25] C. Hu, S. Kong, R. Wang, F. Zhang, and L. Wang, "Insect mass estimation based on radar cross section parameters and support vector regression algorithm," *Remote Sens.*, vol. 12, no. 11, 2020, Art. no. 1903.
[26] A. C. Aldhous, "An investigation of the polarisation dependence of insect radar cross sections at constant aspect," Ph.D. dissertation, Dept. Ecological Physics Res. Group, Cranfield Inst. Technol., Cranfield, U.K., 1989.
[27] T. J. Dean and V. A. Drake, "Monitoring insect migration with radar: The ventral-aspect polarization pattern and its potential for target identification," *Int. J. Remote. Sens.*, vol. 26, no. 18, pp. 3957–3974, 2005.
[28] V. A. Drake, J. W. Chapman, K. S. Lim, D. R. Reynolds, J. R. Riley, and A. D. Smith, "Ventral-aspect radar cross sections and polarization patterns of insects at X band and their relation to size and form," *Int. J. Remote. Sens.*, vol. 38, no. 18, pp. 5022–5044, 2017.
[29] A. D. Smith, J. R. Riley, and R. D. Gregory, "A method for routine monitoring of the aerial migration of insects by using a vertical-looking radar," *Philos. Trans. Roy. Soc. B*, vol. 340, no. 1294, pp. 393–404, 1993.
[30] M. Leskinen, D. Moisseev, and J. Koistinen, "Migrating insects observed by weather radar in traps," presented at the ERAD—the 7th Eur. Conf. Radar Meteorol. Hydrol., Jun. 2012. [Online]. Available: http://www.meteo.fr/cic/meetings/2012/ERAD/extended_abs/NMUR_213_ext_abs.pdf
[31] V. M. Melnikov, M. J. Istok, and J. K. Westbrook, "Asymmetric radar echo patterns from insects," *J. Atmos. Ocean. Technol.*, vol. 32, no. 4, pp. 659–674, 2015.
[32] S. Kong *et al.*, "Insect multifrequency polarimetric radar cross section: Experimental results and analysis," *IEEE Trans. Geosci. Remote Sens.*, vol. 59, no. 8, pp. 6573–6585, Aug. 2021.
[33] K. Sarabandi and F. T. Ulaby, "A convenient technique for polarimetric calibration of single-antenna radar systems," *IEEE Trans. Geosci. Remote Sens.*, vol. 28, no. 6, pp. 1022–1033, Nov. 1990.
[34] F. I. Addison *et al.*, "Simulation of the radar cross section of a noctuid moth," *Remote Sens.*, vol. 14, no. 6, 2022, Art. no. 1494.
[35] M. Li *et al.*, "Influence of channel imbalance on insect orientation estimation in fully polarimetric radar," *J. Signal Process.*, vol. 37, no. 2, pp. 177–185, 2021.

Weidong Li was born in Linyi, Shandong, China, in 1991. He received the B.S. degree in communication engineering and the Ph.D. degree in information and communication engineering from the Beijing Institute of Technology, Beijing, China, in 2015 and 2021, respectively.

Since 2021, he has been a Postdoctoral Researcher with the School of Information and Electronics, Beijing Institute of Technology. His research interests include entomological radar signal processing and radar polarization information processing.

Cheng Hu (Senior Member, IEEE) received the B.S. degree in electronic engineering from the National University of Defense Technology, Changsha, China, in 2003, and the Ph.D. degree in target detection and recognition from the BIT, Beijing, China, in 2009.

He was a Visiting Research Associate with the University of Birmingham, Birmingham, U.K., for 15 months, from 2006 to 2007. Since September 2009, he has been with the School of Information and Electronics, BIT, and promoted to be a Full Professor, since 2014. He has authored/coauthored more than 60 SCI-indexed journal papers and more than 100 conference papers. His research interests include new concept synthetic aperture radar imaging, and the biological detection radar system and signal processing.

Rui Wang was born in Taiyuan, Shanxi, China, in 1985. He received the B.S. degree in information engineering and the Ph.D. degree in information and communication engineering from the Beijing Institute of Technology, Beijing, China, in 2009 and 2015, respectively.

From 2012 to 2013, he was a Visiting Scholar with the Mullard Space and Science Laboratory, University College London, London, U.K. From 2015 to 2017, he was a Postdoctoral Researcher with the Department of Electronics Engineering, Tsinghua University, Beijing, China. Since 2018, he has been an Associate Professor with the School of Electronic Engineering, Beijing Institute of Technology. His research interests include bistatic synthetic aperture radar imaging, stepped-frequency radar signal processing, ISAR imaging, and entomological radar signal processing to extract insect biological parameters.

Dr. Wang was a recipient of the IEEE CIE International Radar Conference Excellent Paper Award, in 2011.

Muyang Li was born in Zhoukou, Henan, China, in 1996. He received the B.S. degree in communication engineering from Hunan University, Changsha, China, in 2018. He is currently working toward the Ph.D. degree in information and communication engineering with the Beijing Institute of Technology, Beijing, China.

His research interests include polarimetric calibration and polarization information processing.

Fan Zhang was born in Chongqing, China. He received the B.S. degree in electronic and information engineering from the Beijing Institute of Technology, Beijing, China, in 2019, where he is currently working toward the Ph.D. degree in information and communication engineering.

His research interests include entomological radar signal processing, electromagnetic scattering research, and target parameter estimation based on machine learning.

Jiangtao Wang was born in Jiyuan, Henan, China, in 1998. He received the B.S. degree in electronic and information engineering from Xidian University, Xi'an, China, in 2020. He is currently working toward the M.A.Sc. degree in information and communication engineering with the Beijing Institute of Technology, Beijing, China.

His research interests include entomological radar signal processing and radar polarization information processing.